JOURNAL OF APPLIED POLYMER SCIENCE VOL. 17, PP. 2329–2354 (1973)

Studies of Converging Flows of Viscoelastic Polymeric Melts. I. Stress-Birefringent Measurements in the Entrance Region of a Sharp-Edged Slit Die

CHANG DAE HAN and LEONARD H. DREXLER, *Department of Chemical Engineering, Polytechnic Institute of Brooklyn, Brooklyn, New York 11201*

Synopsis

Measurements were taken of flow birefringence of viscoelastic polymeric melts in the upstream reservoir and in the entrance region. Materials investigated were polypropylene, high-density polyethylene, and polystyrene. Stress-birefringent patterns, both isochromatics and isoclinics, were formed when a beam of polarized light was sent through a transparent glass cell which consists of a large reservoir and slit die section. Pictures were taken of stress-birefringent patterns, which were later used to obtain quantitative information on the stress distributions of flowing polymeric melts, with the aid of stress optical laws. Also measured were wall normal stresses in the fully developed region, downstream in the thin slit section, which then permitted us to directly determine the stress optical coefficients of the materials tested.

INTRODUCTION

It has long been known that when certain liquids are set in motion, they exhibit the optical characteristic known as "flow birefringence" (doubly refractive properties). When a beam of polarized light is directed at a liquid flowing through a transparent channel and the light leaving the liquid is passed through an analyzer (a piece of polarizing material whose axis of polarization is set at right angles to that of the light entering the liquid), interference patterns become visible which may be related to the magnitude and direction of the shearing stresses set up by the flowing liquid. When monochromatic light is used, regions of light interference and reinforcement result, which appear as a pattern of light and black bands known as *isochromatics*. When white light is used, however, isochromatics appear as bands of the same color. Each band corresponds to a constant value of the maximum shearing stress. Also, when the maximum shearing stress makes a certain angle with the axis of polarization of the incident light, other dark regions occur, known as *isoclinics*. These isoclinics appear only when plane polarized light is employed, whereas the isochromatics appear whether the incident light is plane or circularly polarized.

Lodge[1,2] was the first to suggest that stress birefringence could be used to treat the flow birefringence that occurred in flowing viscoelastic solutions. Extensive experimental work has been conducted by Philippoff[3-6] into extending the stress optical laws for solids to concentrated polymeric solutions. Comprehensive reviews of the molecular theory that has evolved from studies with dilute polymer solutions may be found in Cerf,[7] Janeschitz-Kriegl,[8] and Peterlin.[9] According to these authors, the validity of the stress optical laws for fluids can be checked by plotting the product of the birefringences and the sine of twice the extinction angle against the measured shear stress. The result of such a plot should be a straight line whose slope is the stress optical coefficient. In his review article on flow birefringence, Janeschitz-Kriegl[8] summarizes the work that has been done to confirm that the stress optical laws do apply to polymer systems.

Having determined that the stress optical laws can be utilized for fluids, investigations were conducted in an attempt at solving the entrance region problem. Prados and Peebles[10] developed a method for determining velocity profiles in Newtonian two-dimensional flow, using a highly birefringent milling yellow dye solution. Adams, Whitehead, and Bogue[11] made a birefringent study of a dilute viscoelastic fluid flowing in a 30° converging and diverging channel. They were successful in obtaining point-by-point stress data for this case of accelerated flow. They also showed that the Coleman-Noll second-order theory for viscoelastic fluids correlates their data at low shear rates. Bogue and Peebles[12] have presented a procedure for determining the stress field from optical measurements if the stress optical properties of the fluid are known in simple laminar shearing flow.

Fields and Bogue[13] further investigated the flow of a mildly viscoelastic fluid flowing into a sharp-edged channel. Their experimental shear stresses were in quantitative agreement with those calculated from Weissenberg rheogoniometer data. While correct in magnitude, the normal stresses they obtained were not in agreement with the rheogoniometer results. They were able to show very good detail of the stresses at the entrance area. The entrance region which they found was of the order of one large-channel-diameter width upstream and one small-channel width downstream. An attempt was also made by Fields and Bogue[13] to theoretically describe the upstream accelerated region with the aid of a simplified version of the BKZ theory (Bernstein et al.[14]). Unfortunately, their results only apply to the centerline of the flow.

On the other hand, there have been some efforts[15-19] spent on extending the flow birefringence technique to determine the viscoelastic properties of polymeric melts. Dexter, Miller and Philippoff[15] measured the flow birefringence of molten polyethylene with a standard circular polariscope and parallel-plate viscometer. Wales[17] gives a description of a rectangular-slit apparatus which can be used for the measurement of flow birefringence in molten polymer at relatively high shear rates for fully developed flow. He has reported data for three polymer melts: polystyrene and two polyethylenes. In his review article, Janeschitz-Kriegl[8] explains the technique

of flow birefringence as it applies to viscoelastic polymeric solutions as well as to polymeric melts. For polymeric melts, he describes two experimental apparatuses: (1) a cone-and-plate device where the polarized light beam is directed radially, and (2) a slit rheometer which has a rectangular cross section. The slit instrument is usually preferred because use of the cone-and-plate device is limited to low shear rates.

Unfortunately, at the time when the present study was undertaken, there was no quantitative experimental study reported in the literature on the stress-birefringent patterns of viscoelastic melts in the entrance region, comparable to those studies made of polymeric solutions by Bogue and his co-workers.[11,13] Funatsu and Mori[20] have recently reported their observations on the isochromatics of polyethylene and polypropylene melts flowing into a thin slit die from a large reservoir. However, they did not carry out any quantitative analysis of their observations, and therefore their work was only qualitative in nature.

STRESS OPTICAL LAWS IN FLOW BIREFRINGENCE

In solid photoelasticity it has been a well-established fact that when polarized light enters an optically anisotropic medium, the beam separates into two plane-polarized components in the direction of the principal stresses. When the two components emerge from the medium, they have a certain relative path retardation. Furthermore, under certain conditions extinction of the emerging beam of light occurs, giving rise, when the entire field is viewed, to isoclinic fringe patterns when $2\theta = N\pi$ and to isochromatic fringe patterns when $\alpha/2 = N\pi$. Here, θ denotes the direction of the principal stresses; α, the angular phase difference (or retardation) of the emerging beam of light; and N, an integer.

It has been shown[21-23] that when the direction of a light path is made to coincide with the direction of one of the principal stresses, say σ_3, the relative retardation (or fringe order) R can be related to the difference in the other two principal stresses, $\Delta\sigma$, by

$$\Delta n = C\Delta\sigma \tag{1}$$

where

$$\Delta n = \frac{R\lambda}{d} \tag{2}$$

where d denotes the thickness of the medium and λ the wave length. C in eq. (1) is called the stress optical coefficient measured in Brewsters (1 Brewster = 10^{-13} cm^2/dyne), and Δn is the magnitude of the birefringence. Equation (1) indicates that Δn is a function only of the difference of two principal stresses in the plane perpendicular to the axis of light propagation. Another relationship which is as important in solid photoelasticity as eq. (1) is

$$\theta_{opt} = \theta_{stress} = \theta \tag{3}$$

which indicates that the orientation of the optical axes is identical with that of the principal stress axes. Equations (1) and (3) are called the stress optical laws.

It was Lodge[1] who first suggested that eqns. (1) and (3) may be extended into polymeric solutions. Since then, much work has been done by several researchers to experimentally test Lodge's idea, namely, Philippoff and his co-workers[3-6] and Janeschitz-Kriegl and his co-workers.[8,18] These authors used concentrated polymeric solutions for the most part. Their results showed that the extinction angle measured in birefringence was identical to the orientation of the tensile principal stress calculated from the normal stress measurements. They also showed that the birefringence was proportional to the difference in principal stresses in flow, thus experimentally proving that eqs. (1) and (3) are valid for polymeric solutions also.

It is now seen that the stress optical laws, eqs. (1) and (3), allow for the determination of the principal stress differences from photoelastic measurements. It is possible to transform these stresses from the principal coordinates to the cartesian coordinates by rotation. This transformation[21,23] yields shear stress and difference in normal stresses in terms of principal stresses as follows:

$$\tau_{xy} = \frac{\Delta\sigma}{2} \sin 2\theta_{\text{stress}} \tag{4}$$

$$(\tau_{xy})_{\max} = \frac{\Delta\sigma}{2} = \frac{\tau_{xy}}{\sin 2\theta_{\text{stress}}} \tag{5}$$

$$\tau_{xx} - \tau_{yy} = \Delta\sigma \cos 2\theta_{\text{stress}} \tag{6}$$

Using eqs. (1)–(3), eqs. (4) and (6) may be rewritten as follows:

$$\tau_{xy} = FN \sin 2\theta \tag{7}$$

$$\tau_{xx} - \tau_{yy} = 2FN \cos 2\theta \tag{8}$$

where $F = \lambda/2Cd$. Note that θ is to be obtained from the isoclinic fringe patterns and N from the isochromatic fringe patterns.

However, in order to calculate τ_{yx} and $\tau_{xx} - \tau_{yy}$ from eqs. (7) and (8), the stress optical coefficient C must be known beforehand for the fluid being investigated. It is a well-established fact that the stress optical coefficient for a perfectly elastic material (rubber-like network) is given by[24]

$$C = \frac{(n_0^2 + 2)^2}{n_0} \frac{2\pi}{45} \frac{(\alpha_1 - \alpha_2)}{kT} \tag{9}$$

where n_0 is the mean refractive index of the medium, $\alpha_1 - \alpha_2$ is the difference (or anisotropy) of polarizability of the random link, k is the Boltzman constant, and T is the temperature.

In the present study, however, the determination of the stress optical coefficient C is made from the measurements of τ_{xy}, N, and θ in the well-defined flow field of fully developed flow in the slit, and hence by use of eq. (7).

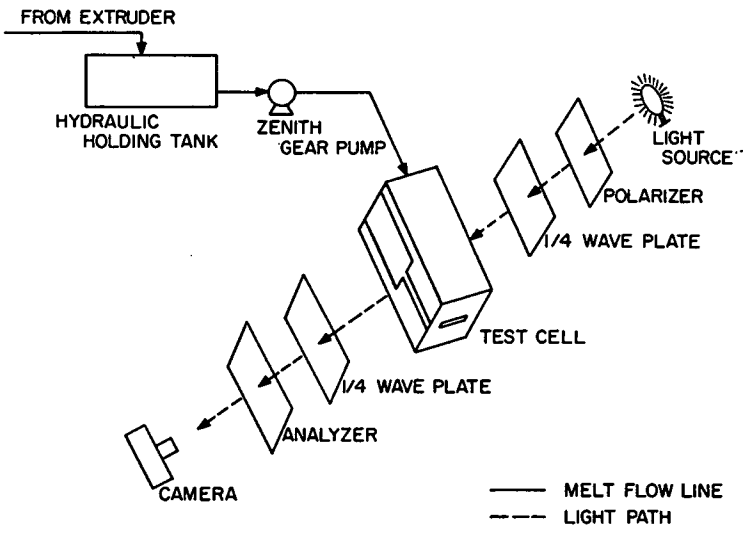

Fig. 1. Schematic diagram of apparatus.

EXPERIMENTAL

The apparatus consists of three major parts: (a) the optical system, (b) the flow test cell, and (c) the polymer melt feed system, as schematically shown in Figure 1.

Optical System

The main components of the optical system are a light source, interference filter, diffusion screen, polarizer, quarter wave plates, analyzer, and a camera.

Two types of light sources were used during the course of this study: a white light source and a monochromatic light source. The white light source was used to obtain colored patterns of the isochromatic fringes. In addition, it allowed for the easy identification of the isoclinic fringes, since these fringes appear as sharp, black bands over the colored isochromatics. Another advantage of using white light is that the zero-order isochromatic fringe always appears black and thus is easily observed. The white light source was a 500-watt incandescent projection-type bulb.

Under the use of monochromatic light, the isochromatic fringes appear as distinct dark bands. These bands can be identified more readily than bands observed under white light. Along with each light source, a piece of flashed opal Plexiglas provided the additional diffusion necessary to produce a uniform light field. In addition, a green monochromatic interference filter was placed between the light source and the observer to insure that the transmitted wavelength was 5461 Å.

The camera for the polariscope was attached to a specially designed camera mount. This mount was made to move to any vertical or horizontal

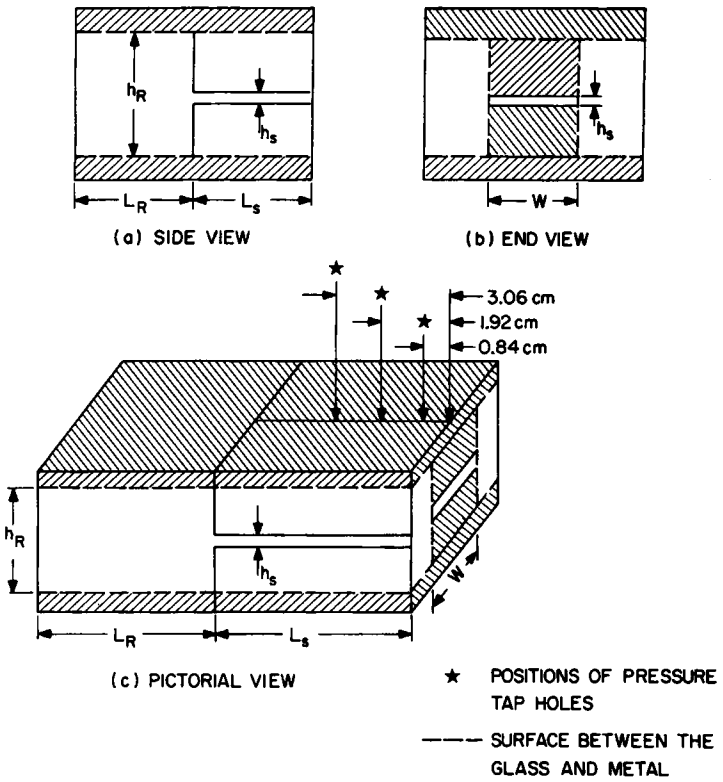

Fig. 2. Schematic diagram of test cells.

position along the optical bench. The camera was a Pentax H3V, 35 mm single-lens reflex, equipped with a 135 mm telephoto lens, a bellows, and 3 closeup lenses (no. 2, no. 3, and no. 10). Kodak Tri-X (ASA 400) film was necessary because of the low-intensity light sources being used.

Test Cells

Two rectangular-slit test cells, hereafter referred to as Test Cell #1 and #2, were designed and built for use in this study. Figure 2 shows views of the test cells used. The cells were made from carbon steel, to the dimensions listed in Table I.

The polymer enters the rectangular-slit die through a 180° sharp-edged entry. In Test Cell #1, the aspect ratio, the ratio of depth-to-width (W/h)

TABLE I
Dimensions of Test Cells

Test cell	h_R, cm	h_S, cm	W, cm	L_R, cm	L_S, cm
#1	2.54	0.199	1.99	2.54	1.58
#2	1.27	0.254	2.54	1.27	5.08

is 10.6:1, and the slit length-to-width (L/h) ratio is 8:1. The selection of this value of the aspect ratio was based on the work of den Otter et al.[16] They showed that wall effects are minimized when the ratio is equal to or greater than 10:1. This cell was designed to study the converging flow section in the upstream reservoir just prior to the entrance to the rectangular slit. In order to minimize the effects of the reservoir walls on this area, the ratio of the upstream width to the slit width was set at 12.8:1. This ratio was not arbitrarily chosen, for Han and Kim[25] have shown the importance of the reservoir-to-capillary diameter ratio on elastic properties of polymer melts flowing through circular tubes. They have found that above a critical value (12:1), the elastic properties are not dependent upon this ratio.

In order to observe the polymer in the entrance region, glass windows were placed on either side of the cell. The windows extended from the beginning of the upstream reservoir to the slit exit. The glass was a strain-free, Vycor glass (No. 7913) manufactured by the Corning Glass Company. The pieces were ground, cut, and polished by the Dell Optics Company of North Bergen, New Jersey, to dimensions chosen so that a maximum working pressure of about 70 kg/cm^2 (a little over 1000 psi) would be realized. The glass plates were bolted to the test cell by means of a steel cover plate, and were separated from the cell and from the cover plate by an asbestos-filled rubber gasket, capable of withstanding 300°C.

All metal surfaces of the test cell were covered with custom-made band and strip mica-insulated electric heaters, manufactured by the Industrial Heater Company, New York, N.Y. The heaters were controlled by means of a Thermistor-regulated temperature controller which had a sensitivity of ±0.5°F. In order to minimize heat losses to the surroundings, a thick layer of asbestos was placed over all the heat surfaces. In addition, a heated chamber was constructed to fit the end of the test cell so as to maintain a uniform polymer temperature inside and immediately outside the cell. Heat losses through the glass windows were reduced by mounting an outside pane over each, with the air trapped between the two acting as an insulator. In order to insure that no temperature gradients existed in the test cell, a pyrometer (Electronic Development Laboratory, Plainview, N.Y., Model MP), equipped with a 5-cm-long needle probe, was employed. With the aid of this unit the melt temperature could be measured at any axial or radial position within the cell.

Whereas Test Cell #1 was designed to study the entrance region, Test Cell #2 was designed to investigate the fully developed rectangular-slit flow region. The aspect ratio of the slit was 10.6:1, which again resulted in a case of one-dimensional flow. The slit length-to-width (L/h) ratio was increased to 20:1. This increase allows for a much longer, fully developed flow region and reduces the chance of the entrance region affecting it. Vycor glass was again used as the windows for the cell. In addition, the same type of heating and temperature control used in Test Cell #1 was employed.

The major difference between the two cells lies in the fact that Test Cell #2 was equipped with three pressure transducers. These transducers, located in the fully developed region (see Fig. 2c for actual location), provided a means for calibrating the birefringence measurements against known physical data.

Polymer Feed System

The polymer melt feed system consisted of an extruder, a holding tank–hydraulic cylinder system, a polymer melt pump, and an electrical heating system, which had been constructed for an earlier study of melt spinning by Han and Lamonte.[26] The extruder is a 1-in.-diameter Killion extruder. The holding tank–hydraulic cylinder combination consists of two Tompkins-Johnson hydraulic cylinders. One cylinder is used as a holding tank for the molten polymer, while the other contains high-pressure oil to force the polymer into the pump inlet. The oil pressure (400–500 psig) is supplied by a hand pump and oil accumulator. The polymer melt pump is a Zenith gear pump which has a rated output of 0.584 cc/rev. The pump, driven by a Link Belt drive unit (HMDG-1), forces the molten polymer through stainless steel tubing into the test cell. It should be noted that the test cell is connected to the optical bench on which the polariscope is attached. Each section through which polymer passes is covered with nichrome wire heaters and, in turn, is insulated with asbestos. The heating system was separated into five sections, each controlled by means of a Thermistor-regulated temperature controller.

Experimental Procedure

The experimental procedure for the flow birefringence measurement was relatively straightforward. The feed system was first preheated to the desired operating temperatures for 4 hr. Polymer pellets were then placed into the extruder, melted, and supplied to the pump reservoir. Oil was then pumped into the oil accumulator until 500 psig pressure was obtained. This pressure forced the melt into the teeth of the Zenith gear pump. The pump was started and set at a predetermined flow rate. Twenty minutes of polymer purging through the test cell was allowed for the flow rate and the temperature to come to equilibrium. At this time, the needle pyrometer was used to ensure that the polymer melt inside the cell was at a uniform temperature. The flow rate was then determined by collecting extrudate samples at specified time intervals. Pressure measurements were then recorded. With the test cell that was positioned directly in the center of the polariscope's light path, birefringent patterns were photographed. Isochromatic fringes were recorded by using circularly polarized monochromatic light (i.e., with the quarter-wave plates in place). The quarter-wave plates were then removed from the light path and isoclinic patterns were recorded using white light. It was necessary to obtain various orientations of the plane-polarized light. This was accomplished by rotating the polar-

izer and the analyzer together, keeping them crossed all the time. The filters were rotated in a counterclockwise direction (when looking at the light source), and photographs were obtained at orientation angles of 0, 10, 20, 30, 40, 50, 60, 70, 80, and 90 degrees. The flow rate was then reset and the procedure repeated.

Wall pressures were measured with Dynisco melt pressure transducers (Model TPT 432). These units are bonded strain gauges with an operating range of 0 to 1500 psig. The metal diaphragm at the tip of the transducer acts as one leg of a Wheatstone bridge. The electrical outputs from the transducers were measured in millivolts with a Leeds and Northrup K-4 potentiometer (Model 7554), and they were balanced with the aid of a Leeds and Northrup (Model 9834) dc null detector. The transducers were calibrated with a dead weight tester at 180°C for the pressure range from 20 to 160 psi. Earlier studies[27,28] indicated that the transducer calibration curve is insensitive to temperature over the range of 180 to 220°C. These instruments had a sensitivity such that the error in measuring the wall pressure was less than 1%. All the transducers were mounted on the cell in a similar manner, as described in earlier papers by Han et al.[27,28] It should be noted that Han[29] has shown that the error due to the pressure hole is for all practical purposes negligible when one is investigating polymer melts.

Materials

Materials used for experiment were: polypropylene (Enjay Chemical, Resin E115), polystyrene (Dow Chemical, Styron 686), and high-density polyethylene (Union Carbide, DMDJ 4309). These polymers had been used on several occasions by Han and his co-workers[30] for the determination of their viscoelastic properties in the molten state.

RESULTS AND DISCUSSION

Isochromatic and Isoclinic Fringe Patterns

Representative pictures of isochromatic fringe patterns are given in Figure 3 for high-density polyethylene at 200°C, in Figure 4 for polypropylene at 180°C and in Figure 5 for polystyrene at 225°C. These pictures were taken using Test Cell #1. It is seen in these figures that the isochromatic fringe patterns strongly depend on flow rate and that the number of fringes increases as the flow rate is increased. Since each band (black and white) corresponds to the locus of points with a constant principal stress difference and also the locus of points of maximum shear stress, one can obtain some important qualitative information by making observations of the isochromatics.

If one is to properly label each of the isochromatic fringes in correct numerical order, it is necessary to know how the fringes develop. While it is not immediately obvious, this information can be obtained, for instance, from the flow rate series shown in Figure 3. The fringes tend to emanate

from the front corners of the slit entrance and develop from the two corners toward the center line of the cell. When these two fringes, which have the same numerical order, meet at the center, they combine with each other. As the flow rate is increased, this combined fringe splits in two and the two parts move simultaneously in different directions. One part of the fringe moves into the slit section and the other moves into the upstream reservoir. In this slit, the fringes tend to straighten out as they move further away from the slit entrance. At the point where the fringes are parallel straight lines, one has left the entrance region and entered the fully developed flow section.

This transition region, where the curved fringes at the entrance move into the slit and become parallel, has been noted previously.[20,31,32] However, Boles et al.[31] did not call this phenomenon a smooth transition; rather, they noted it as a drastic discontinuity in the flow pattern. In their work, Boles

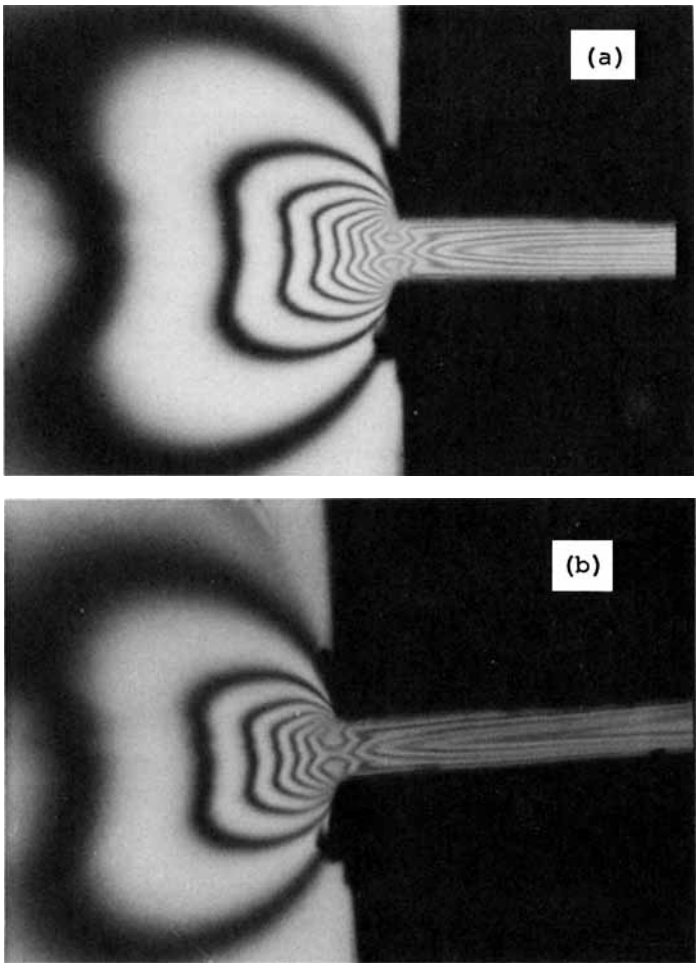

Fig. 3 (*continued*)

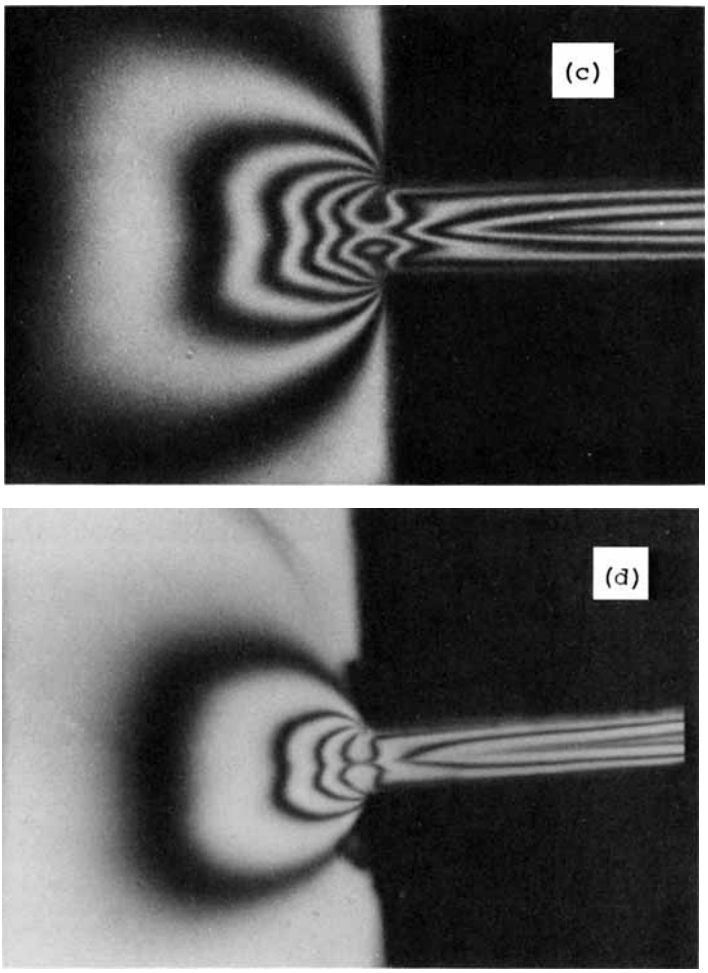

Fig. 3. Isochromatic fringe patterns in the entrance region for high-density polyethylene at 200°C: (a) Q = 17.3 cc/min; (b) Q = 10.9 cc/min; (c) Q = 7.1 cc/min; (d) Q = 3.9 cc/min.

et al. studied the flow of polyisobutylene. This material was not sufficiently birefringent to use the optical technique employed in this study, and a point-by-point method was utilized. Since a point-by-point compensation method does not yield isochromatic patterns but only isoclinic patterns, the smooth transition noted in this study could not be observed.

The other part of the originally combined fringe moves into the upstream reservoir as the flow rate is increased. This fringe grows with a slight curvature on its sides and with a flat center section which contains a small indentation. As the flow rate is increased, this fringe moves further and further away from the slit entrance. The next fringe and, for that matter, all the additional fringes will grow in the same manner as the first fringe.

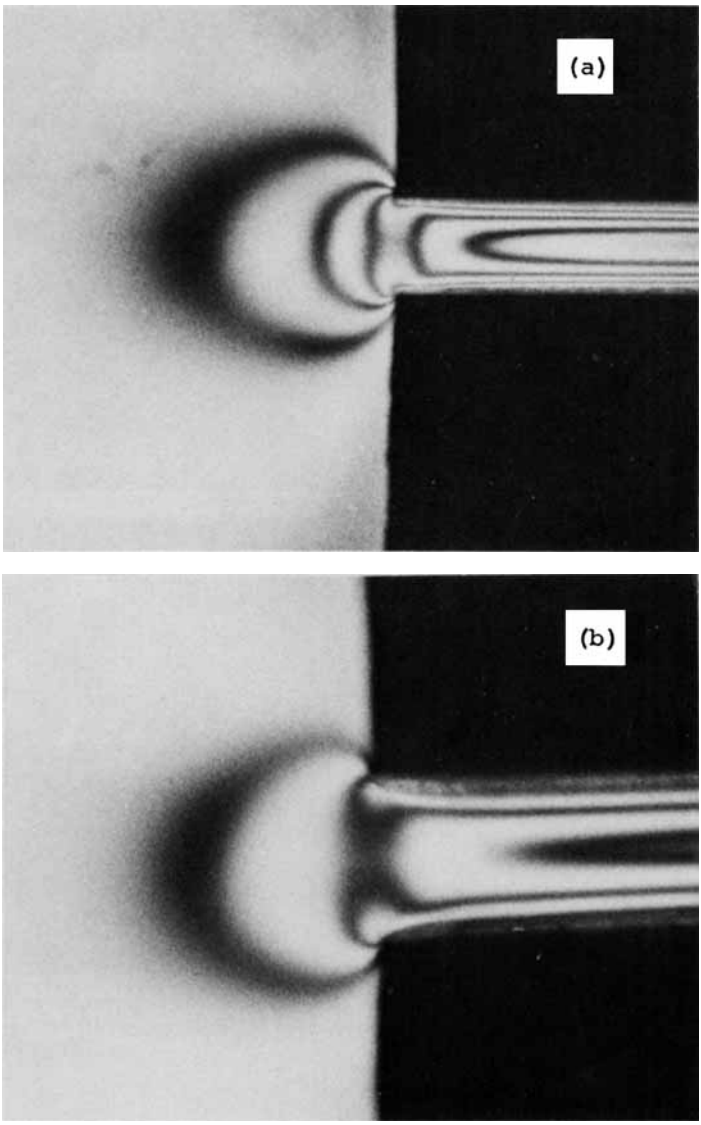

Fig. 4. Isochromatic fringe patterns in the entrance region for polypropylene at 180°C: (a) Q = 26.5 cc/min; (b) Q = 11.5 cc/min.

It is interesting to note that the fringe patterns near the die entrance are characteristic of each material. In other words, the birefringent patterns at the approach to the die entrance and over a short distance from the die entry (i.e., developed flow field) are different for each of the materials tested.

However, despite those differences in the fringe patterns in the entrance region, all materials show the same isochromatic fringe pattern, parallel to the slit die wall, at and beyond the axial position for about twice the slit

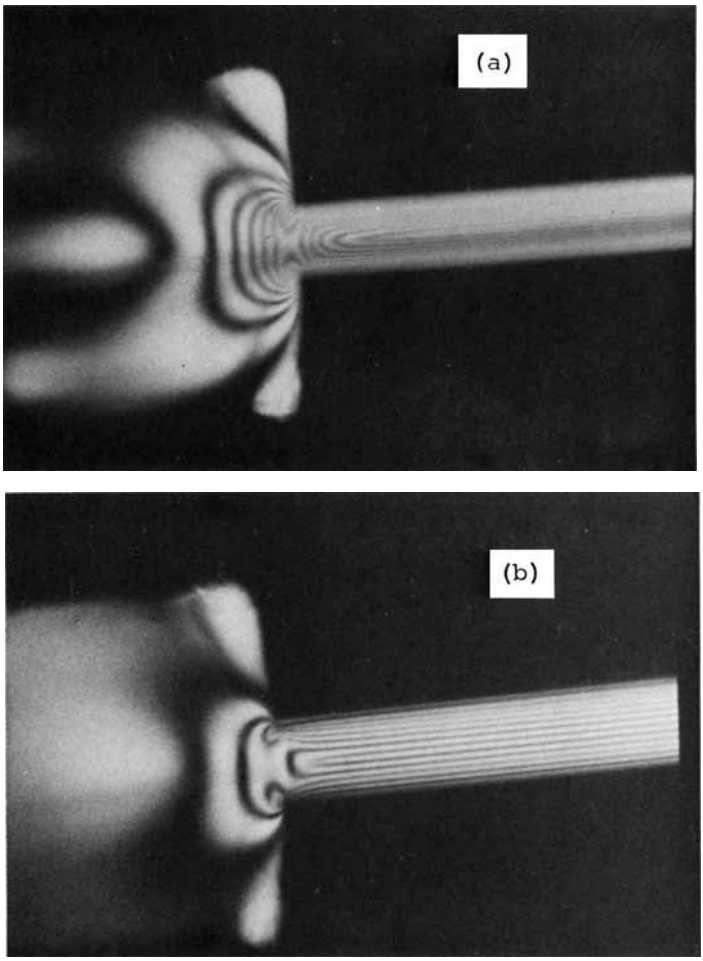

Fig. 5. Isochromatic fringe patterns in the entrance region for polystyrene at 225°C: (a) Q = 18.7 cc/min; (b) Q = 5.5 cc/min.

die thickness. For instance, a close look at the isochromatics in the slit section reveals that, at a distance of about twice the slit thickness from the die entrance, isochromatics become parallel to the slit die wall. This implies that stresses become independent of flow direction. On the other hand, we know from a theoretical point of view that in the fully developed region, shear stress is independent of flow direction, but varies only with the direction perpendicular to the die wall. In the light of this theoretical consideration, the pictures of isochromatics shown in Figures 3 to 5 indicate that the flow becomes fully developed in the slit section at a distance of about two to three times the slit thickness from the die entrance. This conclusion is in agreement with earlier findings by Han et al.,[27,28] who then measured wall normal stresses along the longitudinal direction of capillary dies. It should be noted, however, that a criterion of fully developed flow

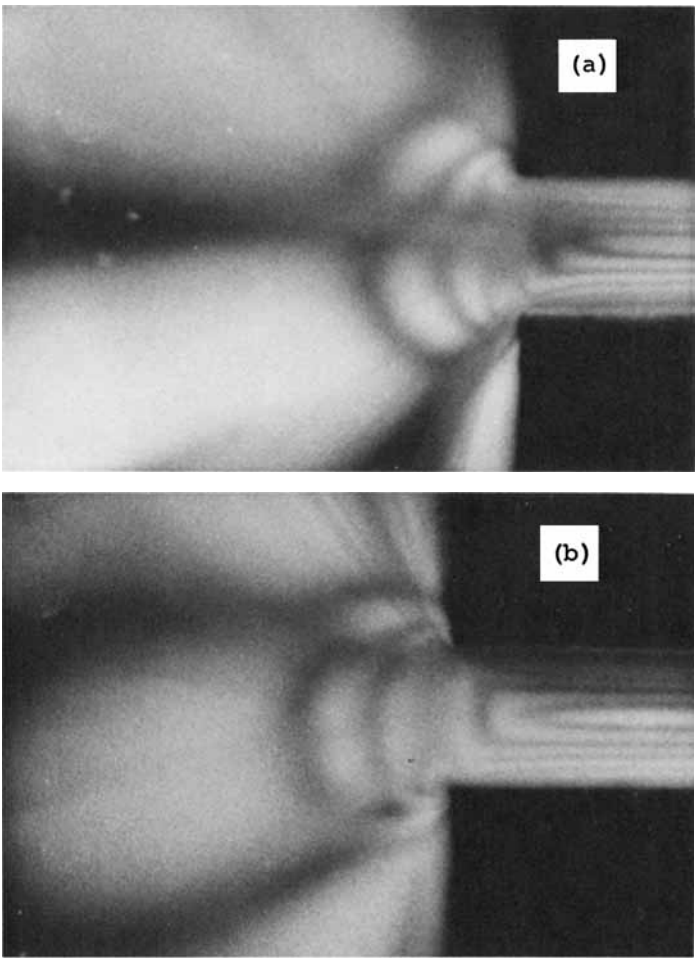

Fig. 6. Isoclinics for high-density polyethylene at 200°C: (a) $\theta = 10°$; (b) $\theta = 60°$.

of viscoelastic materials based on shear stress alone may not be sufficient, as recently discussed by Han and Charles.[33]

Representative isoclinic fringe patterns are given in Figure 6. It should be mentioned that for a given flow rate (i.e., corresponding to one set of isochromatics), as many as nine isoclinics were photographed at rotations of different angles (0 to 90 degrees). Space limitation here does not permit us to present many other pictures taken in our experiment, but a few things are worth mentioning about the pictures of isoclinics.

First, it has been found that isoclinic patterns are not as sensitive to the change in flow rate as isochromotic fringe patterns are. Second, it was found to be virtually impossible to completely eliminate isochromatic fringe patterns when isoclinic patterns were being photographed, whereas the reverse was possible by using circularly polarized light (i.e., in the presence

of quarter-wave plates). However, the presence of the isochromatic patterns was not a severe problem insofar as analyzing the isoclinic patterns was concerned because separate photographs of isochromatic fringe patterns helped isolate the isoclinic patterns.

Determination of Stress Optical Coefficient

In order to obtain quantitative information of local stresses from isochromatic and isoclinic fringe patterns using the stress optical laws, eqs. (7) and (8), it is of utmost importance to accurately determine the stress optical coefficient C. For this, as mentioned above, in the present study measurements were taken of wall normal stresses along the longitudinal direction in the fully developed region of the slit die. Below, we shall describe briefly how the wall pressure measurements enabled us to determine the stress optical coefficient.

Figure 7 gives representative profiles of wall normal stresses of polypropylene at 180°C. Similar profiles were obtained for other materials at various temperatures. From the theoretical point of view, one can show easily that the shear stress τ_{xy} at position y within the slit (see Fig. 2) is given by

$$\tau_{xy} = \left(-\frac{\partial p}{\partial x}\right) y \tag{10}$$

and the shear stress at the wall (i.e., $y = h/2$) by

$$\tau_w = \left(-\frac{\partial p}{\partial x}\right) \frac{h}{2}. \tag{11}$$

Note that $(-\partial p/\partial x)$ is the pressure gradient, which is nothing but the slope of pressure profiles given in Figure 7. Therefore, measurement of wall normal stresses in the slit enables us to construct flow curves (plots of wall shear stress versus shear rate). Figure 8 gives flow curves of the three materials investigated here.

Eliminating $(-\partial p/\partial x)$ from eqs. (10) and (11) gives

$$\frac{\tau_{xy}}{\tau_w} = \frac{2y}{h}. \tag{12}$$

It is now seen that once wall shear stress τ_w is determined, eq. (12) will permit us to determine shear stress τ_{xy} at any position y within the slit.

Figure 9 gives representative pictures of isochromatic fringe patterns in the fully developed region, somewhere 15 to 18 times the slit thickness downstream in Test Cell #2. As briefly mentioned above in connection with the birefringent patterns in the entrance region, the isochromatic fringe patterns downstream of the slit die section are parallel to the die wall, symmetric about the central axis between the two walls. The order of fringes increases with the distance y from the center. Therefore, the fringe order N and the corresponding isoclinic angle θ at the die wall can be

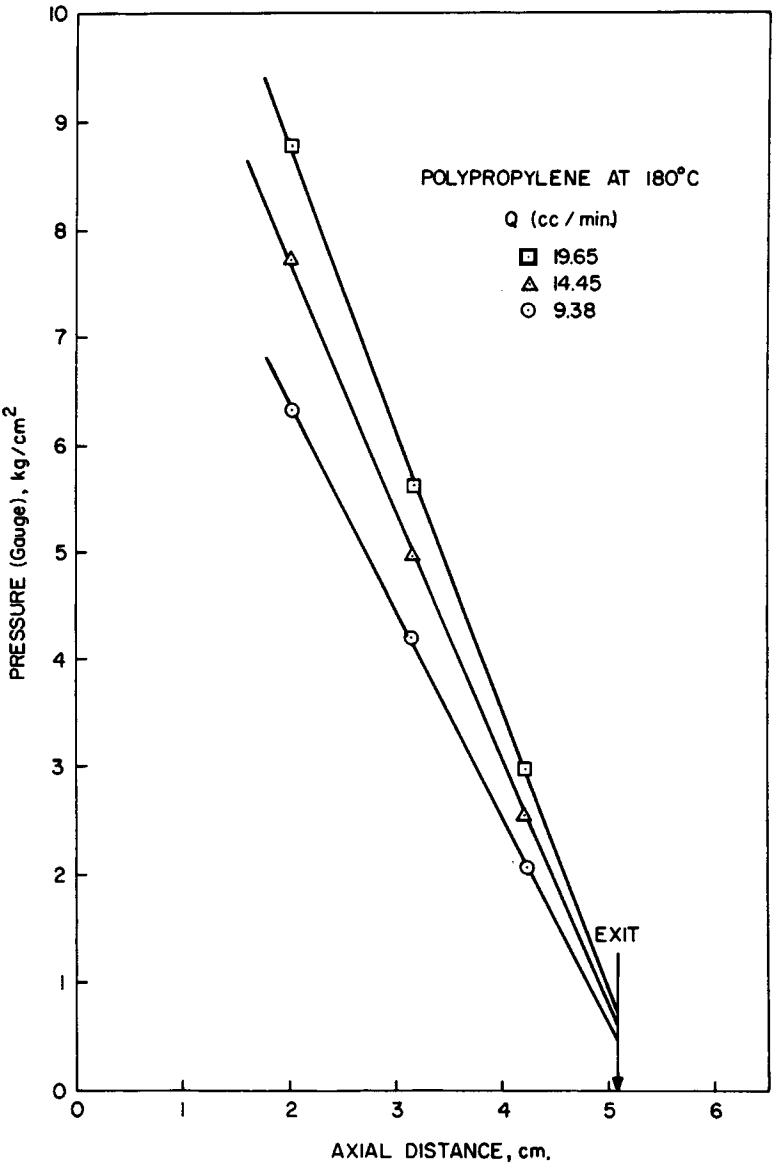

Fig. 7. Representative axial pressure profiles in the fully developed slit flow region for polypropylene at 180°C.

determined by extrapolating the values in the slit (from $y = 0$ to $y < h/2$) to the die wall ($y = h/2$), and by the same token the shear stress τ_{xy} at any position y in the slit can be determined from eq. (12) by knowing the shear stress at the wall, τ_w.

It should be remembered, on the other hand, that eq. (7) suggests that, once the optical stress coefficient C is known, τ_{xy} can be determined from the fringe order, N, and the isoclinic angle, θ. Therefore by combining the

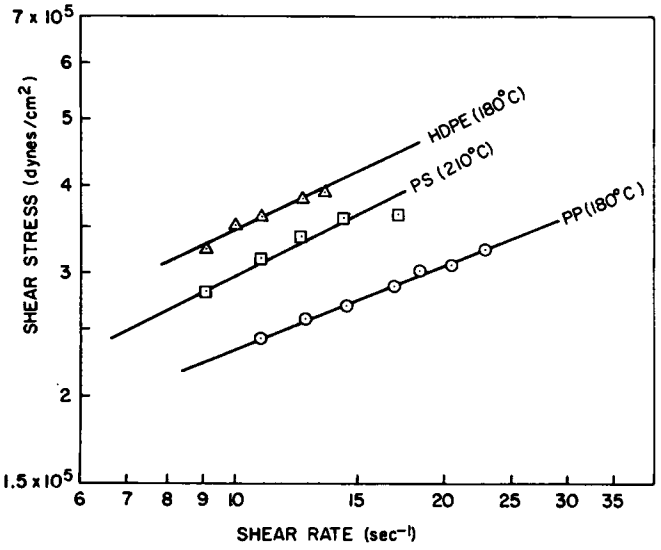

Fig. 8. Plots of shear stress vs. shear rate for the three polymer melts investigated.

shear stress data obtained from the wall normal stress measurement and the shear stress data obtained from the birefringence measurement, i.e., by use of eqs. (7) and (12), the stress optical coefficient C can be determined.

Figure 10 gives plots of τ_{xy} versus N sin 2θ for the three materials investigated. These plots have been prepared by reading off, at different positions y within the slit, the fringe order N from the pictures of isochromatics and θ from the pictures of isoclinics, and calculating τ_{xy} from eq. (12) with the aid of flow curves given in Figure 8. Then, according to eq. (7), the slope of the plots in Figure 10 gives the stress optical coefficient C sought for. Table II gives the stress optical coefficients determined in this study and also values of similar materials reported in the literature.

TABLE II
Stress Optical Coefficients of Polymer Melts

Material	C, (cm²/dyne) $\times 10^{10}$	C, Brewster[a]	Temp., °C	Investigator
High-density polyethylene	1.23	1230	200	this study
	1.60	1600	190	Wales[17]
	1.81	1800	190	den Otter[16]
Polystyrene	4.95	4950	210	this study
	4.10	4100	190	Wales[17]
	−4.89	−4890	196	den Otter[16]
Polypropylene	0.605	605	180	this study
	0.90	900	210	Adamse et al.[19]

[a] 1 Brewster = 10^{-13} cm²/dyne.

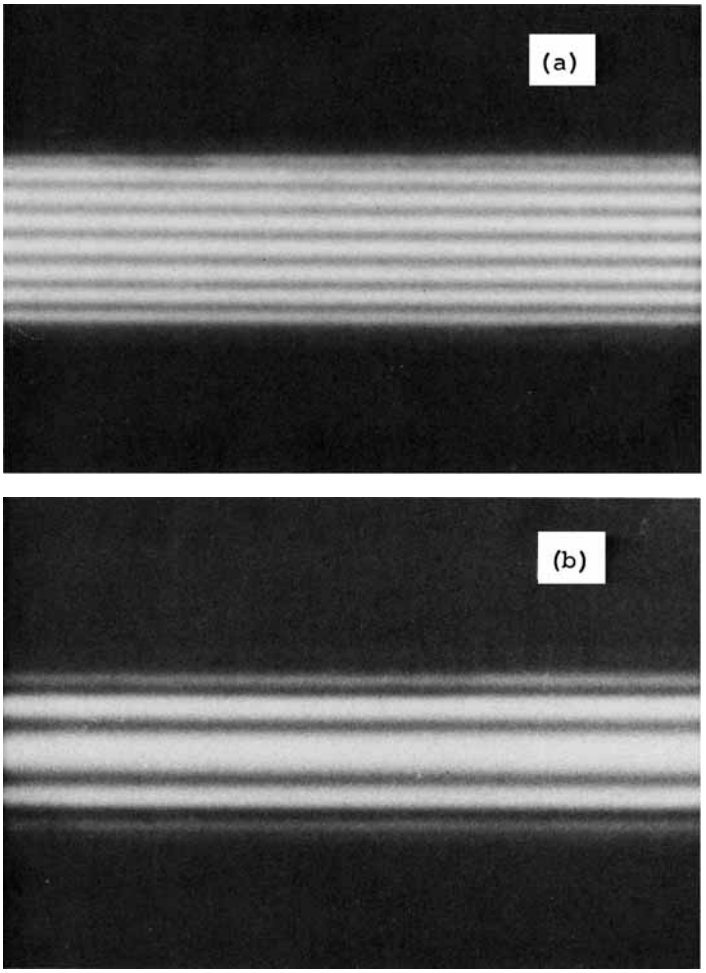

Fig. 9. Isochromatic fringe patterns in the fully developed slit flow region: (a) polystyrene, Q = 4.3 cc/min; (b) polypropylene, Q = 11.5 cc/min.

Considering the differences in molecular distributions of the materials used in this study and by other investigators, the agreement between the values may be said to be quite satisfactory. It should be noted at this point that the fact that plots of τ_{xy} and N sin 2θ give straight lines passing through the origin indicates that the stress optical laws are valid for polymer melts. This is an essential step toward further analyzing the flow birefringence data in the entrance region.

Determination of Stress Distributions

Having recorded both isochromatic and isoclinic fringe patterns in the entrance region and having obtained stress optical coefficients of the mate-

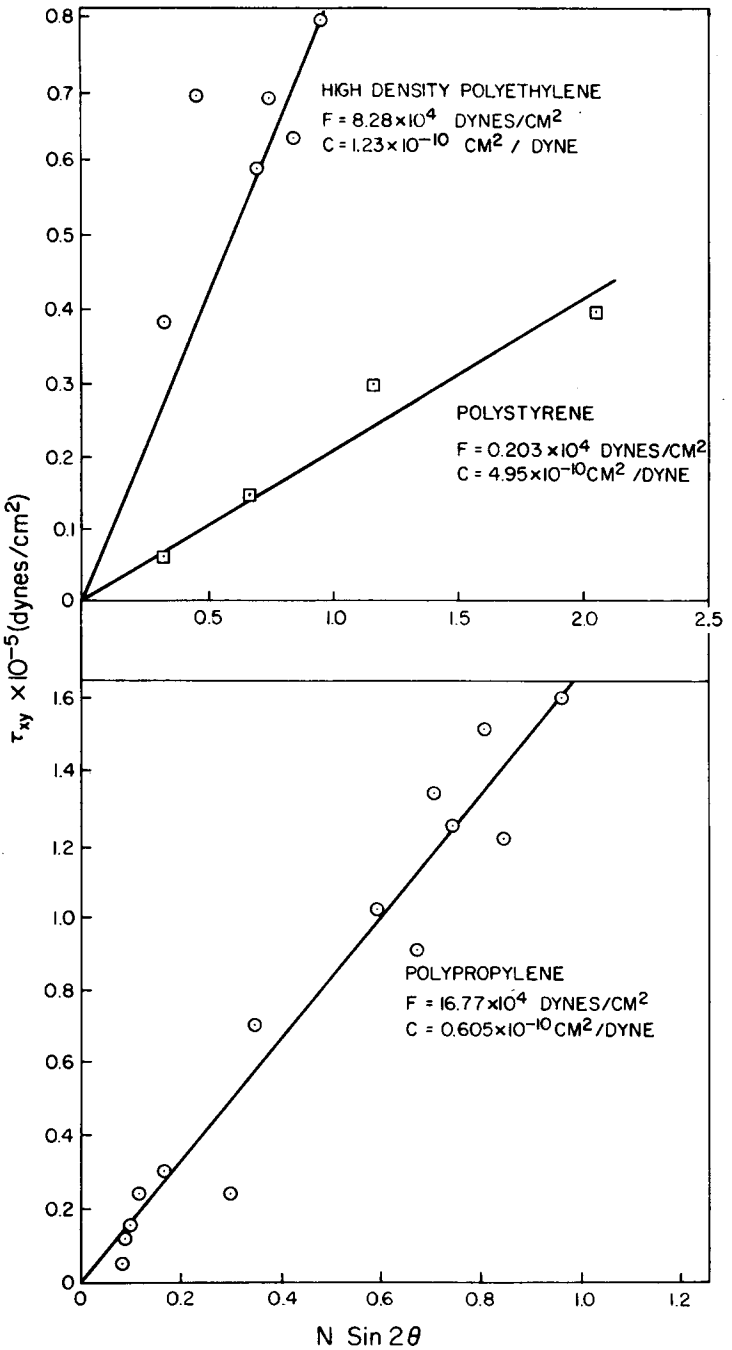

Fig. 10. Plots of τ_{xy} vs. $N \sin 2\theta$ for the three polymer melts investigated.

rials tested, we can now quantitatively determine the distributions of both shear stress and normal stress difference in the converging flow field near the die entrance. We shall briefly outline below the procedures used to obtain point values of stresses in the flow field concerned.

First, in order to accurately read off the fringe orders N and isoclinic angle θ at various positions in the flow field, pictures of isochromatic and isoclinic fringe patterns were first printed on 20 cm $\times$ 25 cm paper with known magnification. Then, a rectangular grid was constructed over the flow region of interest. Only one half of the flow region was analyzed because of the symmetry involved in this type of flow situation. The fringe order N and the isoclinic angle θ were determined at each grid point. This information was then substituted into eqs. (7) and (8).

Once the normal stress difference and the shear stress were known at each grid point, lines of constant stress levels were drawn. A graphic interpolation procedure was devised since the isochromatic patterns did not match the isoclinic patterns at the desired grid points. The technique required that the isoclinic patterns first be combined into one figure representing the family of isoclinics between 0° and 90° in increments of 10°. This was done by tracing the photographic patterns onto one master drawing. It should be noted that the isoclinic lines on the photographs appear as broad, black lines when viewed with white light (see Fig. 6). The broadness of the line is due to the limitation of the film and lens system to resolve the lines properly. In order to trace and record these patterns consistently, a line representing the fringe was drawn through the center of the pattern.

The next step in this data-reduction procedure was to draw horizontal lines at specific vertical positions on both the isochromatic pattern photograph and on the combined isoclinic drawing. The fringe order and its associated horizontal position was then recorded along each of the horizontal lines. In a similar manner, the isoclinic angles and their respective horizontal positions were recorded. It is important to note that all the isochromatic fringe patterns recorded in this study were recorded with the use of a *light* field circular polariscope. The family of isochromatic fringes obtained with this arrangement represents a half order of interference. In order to obtain the fringe order N and isoclinic angle θ at the specific grid points, it was necessary to interpolate between the above recorded positions. This was accomplished by constructing a graph of fringe order versus horizontal position for each horizontal line. A similar procedure was employed for the isoclinic angles also.

It is possible then to obtain the fringe order N and the isoclinic angle θ at specific coordinate positions. This information was then substituted into eqs. (7) and (8) and shear stress and normal stress difference profiles were generated. This final series of calculations was performed on a computer. Distances read from the photographs were converted to actual distances by direct proportion, using the actual slit width to the measured slit width in the photograph as a conversion factor.

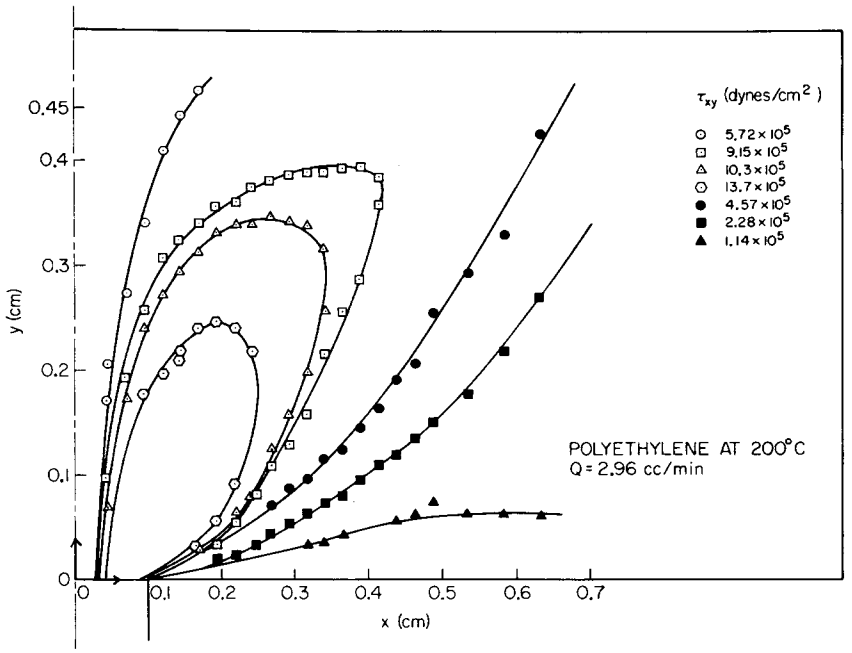

Fig. 11. Shear stress profiles in the entrance region for high-density polyethylene at 200°C.

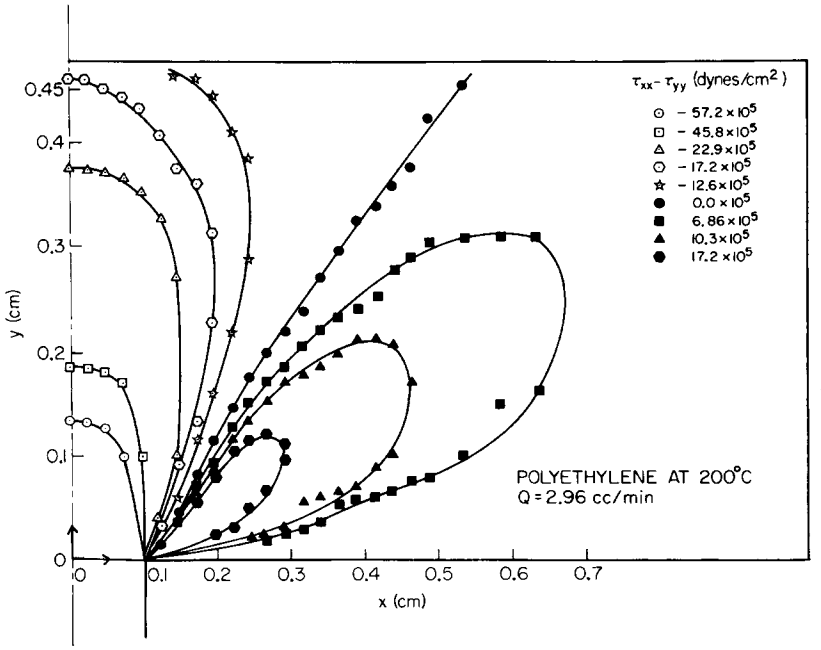

Fig. 12. Normal stress difference profiles in the entrance region for high-density polyethylene at 200°C.

Figures 11 and 12 give distributions of shear stress and normal stress difference, respectively, for high-density polyethylene at 200°C; Figures 13 and 14, for polystyrene at 200°C; and Figures 15 and 16, for polypropylene at 180°C.

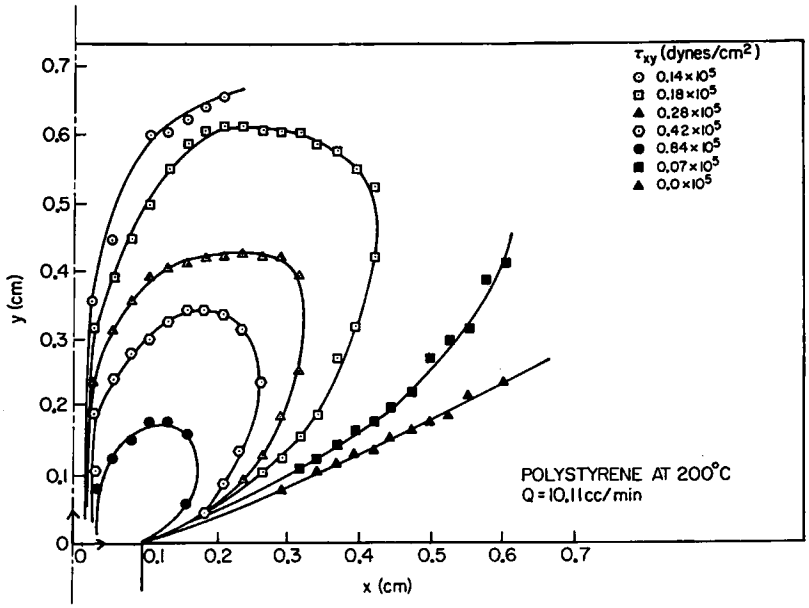

Fig. 13. Shear stress profiles in the entrance region for polystyrene at 200°C.

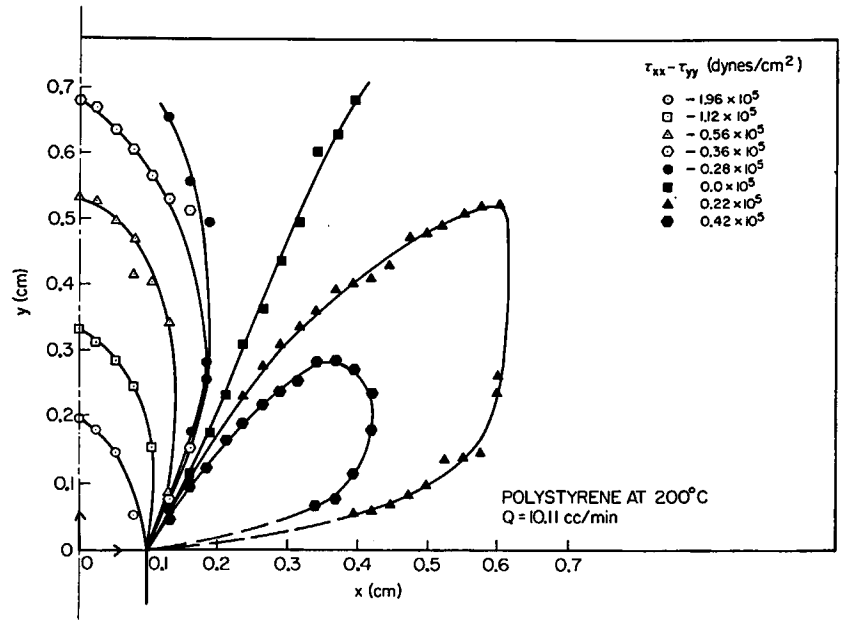

Fig. 14. Normal stress difference profiles in the entrance region for polystyrene at 200°C.

Some comments are in order on the stress distributions given in Figures 11 to 16. First, they are similar, in general features, to those reported earlier by Adams et al.[11] and Fields and Bogue,[13] who used polymeric solutions (10–12% polyisobutylene in decalin). However, because of the low stress levels in the polymeric solutions used by Bogue and his co-workers, they had to take point-by-point measurements of fringe patterns using a laser beam. On the other hand, polymer melts give rise to high stress values, and therefore the use of a readily available polariscope is sufficient to investigate details of the whole flow field with relatively little effort in recording data.

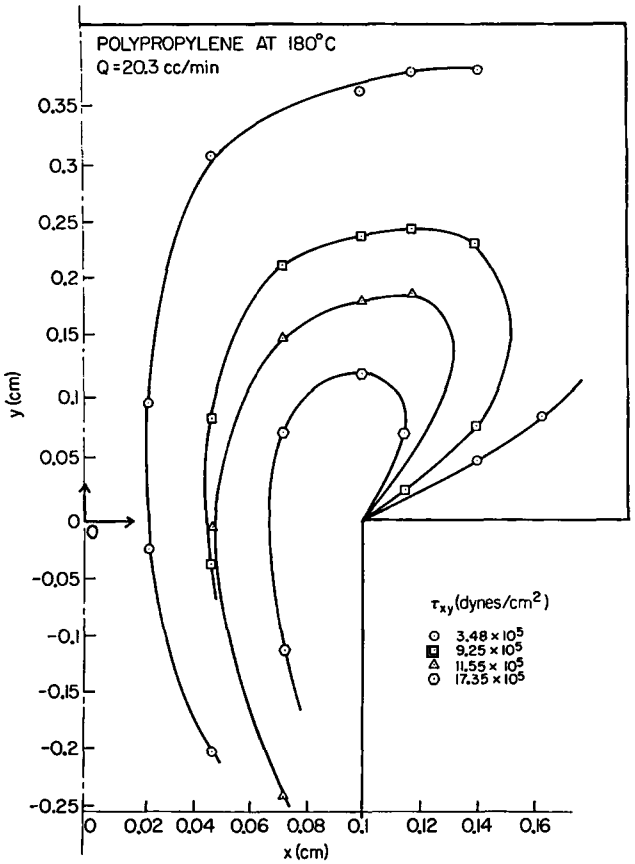

Fig. 15. Shear stress profiles in the entrance region for polypropylene at 180°C.

Second, it should be mentioned that earlier Funatsu and Mori[20] also reported their observations on the isochromatic fringe patterns of polyethylene and polypropylene melts flowing into a thin slit die from a large reservoir. However, they did not carry out any quantitative analysis of their data, and therefore their study was only *qualitative* in nature. As demonstrated in this paper, a quantitative analysis of flow birefringence

data requires the determination of stress optical coefficients and measurements of isoclinics as well, in addition to isochromatic fringe patterns. To the best of the present authors' knowledge, the study reported here appears to be the first attempt ever reported in the literature to quantitatively investigate the stress-birefringent patterns of polymeric melts in the entrance region.

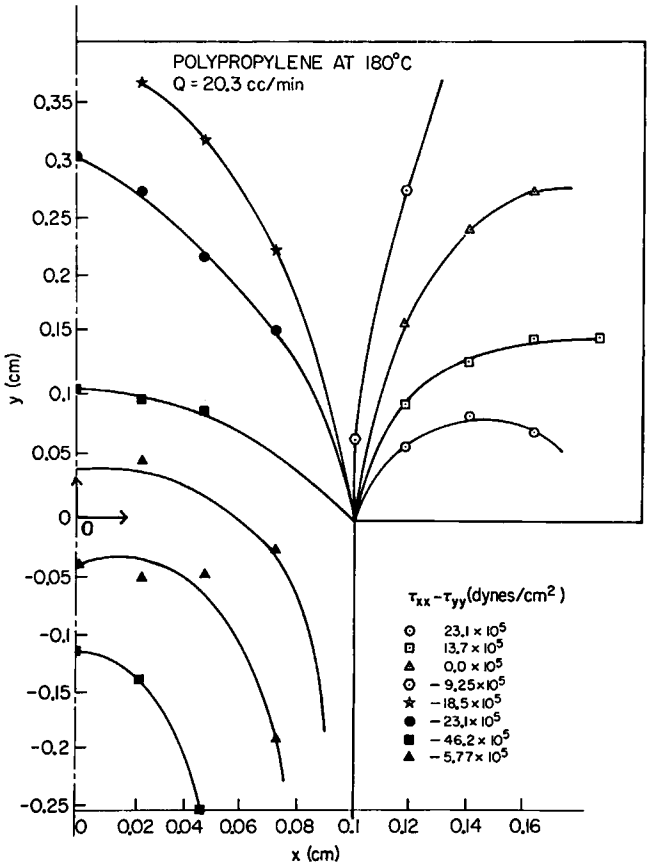

Fig. 16. Normal stress difference profiles in the entrance region polypropylene at 180°C.

Third, in the analysis of the experimental data of the entrance region, an implicit assumption was made that the stress optical laws established in fully developed flow field are also valid in the entrance region. Whether or not such an assumption is valid can be checked if local velocities are also measured in the entrance region and an analysis is carried out to predict stress distributions using viscoelastic constitutive equations.

In a subsequent paper (part II), we shall present an experimental study of local velocity measurements in the converging flow field of tracer particles suspended in flowing polymer melts.

CONCLUSIONS

The following conclusions may be drawn from the present study. First, the isochromatic fringe patterns at the entrance region have provided quantitative information on the entrance length, a point which has long been controversial in the literature. The present paper indicates that, if one uses the stresses as a measure of fully developed flow, the entrance length is about two to three times the slit thickness (or tube diameter) for the three materials investigated and over the range of shear rates investigated.

Second, measurements of wall normal stresses, together with stress-birefringence patterns, have enabled us to determine the stress optical coefficients of the materials investigated, and they are in reasonable agreement with literature values. This has then enabled us to determine, with confidence, the levels of stresses in the flow field concerned. Third, the present paper has given details of the quantitative stress distributions at the entrance region from the pictures taken of isochromatic and isoclinic fringe patterns of viscoelastic polymeric melts.

It can be said that the significance of the present paper lies in that it has demonstrated the usefulness of the flow birefringence technique as a tool for studying details of the stress distributions of rheologically complex polymer melts in the entrance region. Since the flow birefringence technique permits one to make visual observations, it helps one to better understand the process of stress formation in complex flow geometries. Future research will be directed to more complex flow geometries than the one considered in this paper, such as various extrusion dies and molds for blow molding and injection molding processes.

This work was supported in part by the National Science Foundation under Grant GK-23623, for which the authors are grateful. The authors express their thanks to Dr. W. Philippoff who first suggested to them the subject investigated in this paper, and to Professor Sciammarella who helped them interpret the flow birefringence data.

References

1. A. S. Lodge, *Nature*, **176**, 838 (1955).
2. A. S. Lodge, *Trans. Faraday Soc.*, **52**, 127 (1956).
3. W. Philippoff, *J. Appl. Phys.*, **27**, 984 (1956).
4. W. Philippoff, *Trans. Soc. Rheol.*, **1**, 95 (1957).
5. W. Philippoff, *Trans. Soc. Rheol.*, **5**, 163 (1961).
6. W. Philippoff and S. J. Gill, *Trans. Soc. Rheol.*, **7**, 33 (1963).
7. R. Cerf, *Advan. Polym. Sci.*, **1**, 382 (1959).
8. H. Janeschitz-Kriegl, *Advan. Polym. Sci.*, **6**, 170 (1969).
9. A. Peterlin, *Pure Appl. Chem.*, **12**, 563 (1966).
10. J. W. Prados and F. N. Peebles, *A.I.Ch.E.J.*, **5**, 225 (1959).
11. E. B. Adams, J. C. Whitehead, and D. C. Bogue, *A.I.Ch.E. J.*, **11**, 1026 (1965).
12. D. C. Bogue and F. N. Peebles, *Trans. Soc. Rheol.*, **6**, 317 (1962).
13. T. R. Fields and D. C. Bogue, *Trans. Soc. Rheol.*, **12**, 39 (1968).
14. B. Bernstein, K. Kearsley, and L. Zapas, *Trans. Soc. Rheol.*, **7**, 391 (1963).
15. F. D. Dexter, J. C. Miller, and W. Philippoff, *Trans. Soc. Rheol.*, **5**, 193 (1961).

16. J. L. den Otter, Doctoral Dissertation, University of Leiden, 1967.
17. J. L. S. Wales, *Rheol. Acta*, **8**, 38 (1969).
18. J. L. S. Wales and H. Janeschitz-Kriegl, *J. Polym. Sci. A-2*, **5**, 781 (1967).
19. J. W. C. Adamse, H. Janeschitz-Kriegl, J. L. den Otter, and J. L. S. Wales, *J. Polym. Sci. A-2*, **6**, 871 (1968).
20. K. Funatsu and Y. Mori, *Chem. High Polym.* (Japan), **25**, 337 (1968).
21. M. M. Frocht, *Photoelasticity*, Vol. 1, Wiley, New York, 1941.
22. A. J. Durelli and W. F. Riley, *Introduction of Photomechanics*, Prentice-Hall, Englewood Cliffs, N.J., 1965.
23. A. W. Hendry, *Photoelastic Analysis*, Pergamon Press, New York, 1966.
24. L. R. G. Treloar, *The Physics of Rubber Elasticity*, 2nd ed., Oxford Press, London, 1958.
25. C. D. Han and K. U. Kim, *Polym. Eng. Sci.*, **11**, 395 (1971).
26. C. D. Han and R. R. Lamonte, *Trans. Soc. Rheol.*, **16**, 447 (1972).
27. C. D. Han, M. Charles, and W. Philippoff, *Trans. Soc. Rheol.*, **13**, 455 (1969).
28. C. D. Han, M. Charles, and W. Philippoff, *Trans. Soc. Rheol.*, **14**, 393 (1970).
29. C. D. Han, *A.I.Ch.E.J.*, **18**, 116 (1972).
30. C. D. Han, K. U. Kim, N. Siskovic, and C. R. Huang, *J. Appl. Polym. Sci.*, **17**, 95(1973).
31. R. L. Boles, H. L. Davis, and D. C. Bogue, *Polym. Eng. Sci.*, **10**, 24 (1970).
32. T. R. Fields, M. S. (Ch.E.) Thesis, University of Tennessee, Knoxville, Tennessee, 1967.
33. C. D. Han and M. Charles, *A.I.Ch.E. J.*, **16**, 499 (1970).

Received October 6, 1972
Revised December 12, 1972